Nonlinear multi-scale homogenisation with different structural models at different scales

B. D. Edmans[1]*, G. Alfano[1], H. Bahai[1]

August 15, 2014

[1]School of Engineering and Design, Brunel University, Kingston Lane, Middlesex, UB8 3PH, UK

Abstract

We present an extension of the computational homogenisation theory to cases where different structural models are used at different scales and no energy potential can be defined at the small scale. We observe that volumetric averaging, that is not applicable in such cases unless similarities exist in the macro- and micro-scale models, is not a necessary prerequisite to carry out computational homogenisation. At each material point of the macro-model we replace the conventional representative volume element with a representative domain element (RDE). To link the large- and small-scale problems we then introduce a linear operator, mapping the smooth part of the small-scale displacement field of each RDE to the large-scale strain field, and a trace operator to impose boundary conditions in the RDE. The latter is defined based on engineering judgement, analogously to the conventional theory. A generalised Hill's condition, rather than being invoked, is derived from duality principles and is used to recover the stress measures at the large scale. For the implementation in a nonlinear finite-element analysis 'control nodes' and constraint equations are used. The effectiveness of the procedure is demonstrated for three beam-to-truss example problems, for which multi-scale convergence is numerically analysed.

*Corresponding author. E-mail: benjamin.edmans@brunel.ac.uk

1 Introduction

Multi-scale methods are an increasingly used approach in a wide range of applications in computational mechanics thanks to the continuous increase in computer memory, speed and power, the impressive advances of hardware, software and algorithms for parallel computing and the further developments of the underlying multi-scale homogenisation theories of the last decade, particularly for nonlinear problems.

Many basic multi-scale methods have found their earliest expression in composites modelling and associated statistical averaging techniques (for a survey of such techniques, see e.g. Hashin [1]). Representative Volume Element (RVE) -based methods, first proposed by Hill [2], involve the creation of a single representative model of a portion of a complex material or structure, chosen and/or constructed such that its analysis yields accurate estimates of the large-scale stress-strain behavioural parameters in the vicinity of any given point in the large-scale model. RVEs are required to be large enough that they incorporate the heterogeneities (inclusions, voids, etc.) on the scale at which they occur, but small enough that the 'coarse-graining' of the material response does not lead to significant inaccuracies in the predicted behaviour of the large-scale model.

A widely used development from RVE techniques leads to computational homogenisation methods. In a finite-element-based parallel or concurrent computational homogenisation procedure, strains resulting from an attempted displacement increment are calculated at each integration point in the large-scale model. Each set of strains at each integration point is imposed on a separate RVE model and the resulting stresses are averaged over the RVE and returned to the integration point in the large-scale model for residual calculation. Such methods are conceptually straightforward and can be applied to nonlinear problems [3, 4], though their efficiency in localisation is variable and the computational expense of the nested solution procedure can be considerable.

The displacement field in the RVE is typically decomposed into a smooth part and a locally fluctuating part. A key aspect of the formulation is that the smooth part is directly linked to the macro-strain, while boundary conditions are applied to the fluctuating part. Common boundary

conditions choices include the so-called Taylor assumption of zero fluctuations, uniform displacement, periodic displacement, uniform traction and mixed traction-displacement boundary conditions [5, 6]. For typical applications, it has been shown that periodic boundary conditions are more accurate for predicting bulk material behaviour than the uniform types [6, 7, 8, 9].

A concurrent computational homogenisation is a computationally expensive procedure, a feature that is often aggravated by lack of convergence of the iterative procedure used at the small-scale model, especially if the small-scale model incorporates nonlinear behaviour. For this reason, a sub-stepping approach has been suggested by Perić *et al*. [10] to provide better estimates of the RVE configuration.

Applications of computational homogenisation in the literature mostly involve transfer of field quantities between scales where continuum models are used. In the so-called first-order framework, Cauchy models are used at all scales and averaging principles are used to transfer field quantities from one scale to the other. In particular, the macro-strain and macro-stresses are assumed to be the average on the RVE of the corresponding micro-strain and micro-stresses.

A limitation of the first-order computational homogenisation method lies in the enforcement of a uniform macro-strain across the RVE which may not be an adequate representation in situations where strain localisation or fracture occurs. To remedy this, non-local continuum models such as Cosserat or strain-gradient models may be used. Examples of such procedures are given in the papers by Kouznetsova *et al*. [11] and Kaczmarczyk *et al*. [12], who use second-order macro-continua and first-order micro-continua to investigate the effect of the micro-structure size, and by Addessi *et al*. [13] and by Adessi and Sacco [14] who analyse masonry walls in the framework of transformation field analysis using two-dimensional Cosserat continuum models for large-scale modelling, while the small-scale model of masonry incorporates a nonlinear damage contact-friction model for the mortar joint.

In these cases, the models used at either scale are not the same. Hence, to relate the deformation at the micro-scale to the first and second order strain measure at the large scale, suitable extensions of the averaging principle are formulated by Kouznetsova *et al*. [11] and Kaczmarczyk *et al*. [12] whereas Adessi and Sacco used a least-square optimisation procedure to minimise the

difference between macro-displacement and the smooth field at the small scale. To recover the stress measures at the large scale the Hill-Mandel condition, which states that the corresponding micro- and macro- virtual works should be the same, is invoked. Since the models at both scales are different but still both continuum, they are able to ultimately compute the stress tensors at the macro-scale through integral expressions of the micro-stress field, either over the RVE volume or on its boundary.

Examples of nonlinear computational homogenisation in which a continuum model is used at the small scale while a structural model is used at the large scale is contributed by Geers *et al.* [15] and Coenen *et al.* [16] who develop a formulation for heterogeneous thin sheets using continuum shell elements at the macro-level and continuum elements at the micro-level. In this approach, a second order approximation to the nonlinear deformation map is used, with components of the deformation gradient and second deformation gradient identified as shell generalised strain measures. Stress resultants are recovered from the detailed model by integration of the continuum strains over the RVE transverse faces, equivalent to a form of volumetric averaging.

Multi-scale techniques have been developed to bridge atomic- and microscopic- scale representations of materials. This requires linking continuum and atomistic models and therefore also represents an example in which different types of model are used at different length scales. Computational homogenisation principles can also be applied here. An example of this is demonstrated by Samadikhah *et al.* [17] in the modelling of graphene membranes. In this article, computational homogenisation relations were used to express atomic displacements as a function of the macro-scale displacement field and deformation gradient. A total potential energy functional is calculated by summing interatomic potentials calculated using the local displacement fluctuation field. The sum of energy-conjugated atomic forces is used to calculate the microscopic stress, via the principle of equivalence of micro- and atomic-scale internal work. This approach clearly can only be used for problems where an energy functional exists.

An alternative approach to computational homogenisation, described by da Cruz *et al.* [18], Hassani and Hinton [19], Guedes and Kikuchi [20] and others, is the asymptotic expansion method. The two-scale asymptotic method expresses the displacement field as a power se-

ries expansion with coefficients that are increasing powers of the scaling parameter (a constant representing the ratio between characteristic length scales of the microscopic and macroscopic problems), multiplying component displacement functions that are periodic with a period equal to the RVE length. This converts the original boundary value problem into a pair of closed-form boundary value problems to be solved sequentially for the first-order solution. Higher order periodic components of the displacement may be calculated up to an arbitrary level of accuracy using higher order equation sets resulting from the original boundary value problem (BVP) expansion. For linear problems (used by, for example, Guedes and Kikuchi [20]), only one boundary value problem needs to be solved at each scale (for a first order approximation): a small-scale simulation to determine the homogenised elastic operator which completely characterises its behaviour, and a large-scale simulation to address the problem of interest. RVE geometries, as for other homogenisation methods, are usually parallelepipeds, though Ghosh *et al.* [21] adapts the technique to the Voronoi cell finite element method, which uses an irregular polygonal tessellation of the plane, such that each macro-scale contains at most a single secondary-phase inclusion.

The asymptotic expansion method has also been extended to solve nonlinear problems. This requires a nested solution scheme. Fish and Shek [22] present a three-scale nonlinear asymptotic method solved using a specialised multi-scale Newton-Raphson solution algorithm, along with a derivation of the associated error estimators.

Most of the work done on asymptotic expansion techniques expand the governing (continuum) partial differential equations (PDE) and express the resulting equation sets in continuum form. In this way, as in the case of computational homogenisation, homogenisation between the same continuum models, rather than different continuum or structural models, is dominant. An extension using a large-scale structural model includes the development for general linear periodic beams in bending by Buannic and Cartraud [23]. Multi-scale algorithms for general (linear and nonlinear) RVEs may also be developed using variational formulations by using the concept of two-scale convergence. This approach has been explored by Terada and Kikuchi [24].

In this paper, we present a general extension of the conventional multi-scale homogenisation theory, developed for the case when the same, typically continuum, models are used at either

scale, to the general case when different and arbitrary structural models are used at each scale. The necessity of such extended theory, which does not require the existence of an energy potential at the small scale, emerged during the development of multi-scale models for flexible risers [25, 26, 27]. The proposed formulation provides a general framework which can be applied to a wide range of cases, including, among others, the cases of 2D or 3D truss structures that at a very large scale can be modelled as beams or shells, but also problems where higher-order continua are used at the macro-scale and a Cauchy continuum model is used at the micro-scale, such as for the second-order computational homogenisation. In all these cases, the conventional theory based on strain and stress averaging is not applicable, at least, not directly, because its implicit requirement is that the same formal model is used at both length scales, or, at least, that it is possible to compute some local value that represents the macro-generalised-strain or the macro-stress resultants on the RVE, that can be integrated over the remaining dimensions of the RVE.

An original and more general theoretical justification of how the micro-scale BVP is defined starting from the macro-strain is provided. Since our theory is not restricted to solid continua we introduce at each point of the macro-domain a representative domain element (RDE) instead of a RVE. We show that averaging principles are neither sufficient nor necessary to define boundary conditions on the RDE and construct our extended theory by reformulating the donw-scaling procedure, to obtain the micro-scale displacement field from the macro-strain, in terms of general operators not dependent on the specific continuum or structural models used. The up-scaling procedure to recover macro-stresses from the micro-stress field in each RDE is based on a generalised Hill's condition obtained from general duality principles of structural mechanics.

An application of this extended theory is presented for the fully nested (FE^2) multi-scale nonlinear analysis of a truss for which each member is treated as elasto-plastic. The relative simplicity of this problem allows the fundamental theoretical contributions of the paper to be highlighted and makes it possible to assess the effectiveness of the proposed approach by comparison of the results of the multi-scale method with those of direct numerical simulations. A similar problem has previously been studied by Tollenaere and Caillerie [28]. An application of

such a model could be in modelling auxetic foams, where analytical calculations are often used to determine unit cell behaviour (see e.g. Smith *et al.* [29]), but a multi-scale approach could bring benefits.

An outline of the paper is as follows: firstly, the theory of the first-order computational homogenisation method is extended to a more general structural-structural procedure in a general form (Section 2). This is followed in Section 3 by descriptions of the form of the large-scale (Section 3.1) and small-scale (Section 3.2) models chosen for our specific application, the latter including details of the implementation of the homogenisation procedure derived from theoretical considerations. Numerical results and the validation of the multi-scale model predictions against the results of direct numerical simulations are reported and discussed in Section 4. Finally, summarising remarks on the method and its application are made, with a view to future further developments.

2 Structural-structural homogenisation

2.1 Conventional computational homogenisation procedure

In this section we review the conventional two-scale computational homogenisation procedure developed for the case where the same continuum-based model is used at both scales, using the same continuum stress and strain measures. We conclude the section by explaining why the formulation cannot be directly applied to the more general case when different models are used at different scales, and by making a number of remarks which suggest and justify the generalisation proposed in Section 2.2.

For simplicity, this review is limited to the case of the first-order homogenisation and small strains and displacements. Higher-order and/or geometrically nonlinear formulations can be obtained using similar arguments.

The starting point is the assumption of 'separation of scales', whereby at each point x_M of the macro-domain Ω under consideration a representative volume element (RVE) is postulated to exist and to occupy a domain Ω_{RVE} typically (but not necessarily) centred on x_M, such that

the RVEs associated with two points with arbitrary separation are treated as independent (even if they overlap). The microscopic displacement u_m in the RVE is expressed as the sum of a smooth component v_m and a fluctuating component w_m:

$$u_m(x_m, x_M) = v_m(x_m, x_M) + w_m(x_m, x_M) \tag{1}$$

where $x_m \in \Omega_{RVE}$. The smooth component describes a displacement field in the RVE which is linear in x_m so that its associated strain is constant within Ω_{RVE} and is equal to the macroscopic strain $\varepsilon_M(x_M)$:

$$\varepsilon_M(x_M) = \nabla_s v_m(x_M) \tag{2}$$

where ∇_s is the symmetric part of the gradient. Therefore, the microscopic strain ε_m can also be decomposed as follows:

$$\begin{aligned} \varepsilon_m(x_m, x_M) &= \nabla_s v_m(x_M) + \nabla_s w_m(x_m, x_M) \\ &= \varepsilon_M(x_M) + \nabla_s w_m(x_m, x_M) \end{aligned} \tag{3}$$

The constitutive law and the equilibrium differential equations are then imposed on the RVE:

$$\begin{cases} \sigma_m(x_m, x_M) = \sigma_m[\varepsilon_m(x_m, x_M)] \\ \\ \operatorname{div} \sigma_m(x_m, x_M) = 0 \end{cases} \tag{4}$$

where for simplicity (and without loss of generality) we assume that inside the RVE there is no significant fluctuation of the body forces, which therefore can be neglected.

The following assumption is then made:

$$\varepsilon_M(x_M) = \overline{\varepsilon_m}(x_M) \tag{5}$$

where the bar indicates the average over the RVE:

$$\overline{(\bullet)_m}(x_M) = \frac{1}{\Omega_{RVE}} \int_{\Omega_{RVE}} (\bullet)_m(x_m, x_M) \, \mathrm{d}\Omega_{RVE} \tag{6}$$

Integrating the microscopic strain ε_m over the RVE and using Equations (3) and (6) and the Green theorem, the following relation is obtained:

$$\oint_{\partial\Omega_{RVE}} w_m(x_m, x_M) \otimes N(x_m)\, \mathrm{d}\partial\Omega_{RVE} = 0 \qquad \forall\, x_M \in \Omega \tag{7}$$

N denoting the normal to the boundary of the RVE.

The above equations provide a method to determine a micro-displacement field on the RVE starting from a known deformation at the macro-scale (so-called 'down-scaling' procedure [12]): given a macro-strain field ε_M, a micro-displacement field u_m can be determined by solving, in each RVE, the boundary value problem (BVP) represented by Equations (1)-(4) and a suitable set of boundary conditions respecting Equation (7). It has been shown that boundary conditions which comply with Equation (7) include zero fluctuations over the whole RVE (Taylor assumption), uniform displacement, uniform traction and periodic boundary conditions (see, for example, Larsson *et al.* [30] and Peric *et al.* [5]). The latter have been found to be the most effective for most cases involving a periodic microstructure or when the microstructure is not periodic but the RVE is sufficiently statistically representative [7, 31].

Once the above BVP is solved for each RVE, the macro-stress field is recovered by averaging the micro-stress field over the RVE (so-called 'up-scaling' procedure [12]):

$$\sigma_M(x_M) = \overline{\sigma_m}(x_M) \tag{8}$$

This stress-averaging procedure is related to Hill's condition, which, in one of its forms, states that the local macroscopic virtual work done by the macroscopic stress for any macroscopic strain variation must be equal to the average over the RVE of the microscopic virtual work done by the microscopic stress for the corresponding microscopic strain variation [11, 32]:

$$\sigma_M \cdot \delta\varepsilon_M = \overline{\sigma_m \cdot \delta\varepsilon_m(\delta\varepsilon_M)} \qquad \forall \delta\varepsilon_M \tag{9}$$

where dependence on the local and global position will henceforth be omitted in the notation for simplicity. The notation $\delta\varepsilon_m(\delta\varepsilon_M)$ highlights that the microscopic strain variation $\delta\varepsilon_m$ is the

variation of the solution to the BVP (given in terms of the microscopic strain) corresponding to a variation $\delta\varepsilon_M$ of the macroscopic strain ε_M. From Equations (2) and (3):

$$\delta\varepsilon_m(\delta\varepsilon_M) = \delta\varepsilon_{mv} + \delta\varepsilon_{mw} = \delta\varepsilon_M + \delta\varepsilon_{mw} \tag{10}$$

where $\delta\varepsilon_{mv} = \delta\nabla_s v_m$ and $\delta\varepsilon_{mw} = \delta\nabla_s w_m(\delta\varepsilon_M)$. In the absence of body forces the self-equilibrated microscopic stress field on the RVE is orthogonal to the field $\delta\varepsilon_{mw}$, i.e. it results that

$$\int_{\Omega_{RVE}} \sigma_m \cdot \delta\varepsilon_{mw}\, d\Omega = 0 \tag{11}$$

which leads to:

$$\begin{aligned} &\overline{\sigma_m \cdot \delta\varepsilon_m(\delta\varepsilon_M)} = \frac{1}{\Omega_{RVE}} \int_{\Omega_{RVE}} \sigma_m \, \mathrm{d}\Omega \cdot \delta\varepsilon_M = \\ &= \overline{\sigma_m} \cdot \delta\varepsilon_M \qquad \forall\delta\varepsilon_M \end{aligned} \tag{12}$$

Hence, assuming that Relation (8) holds true, then from Equation (12), Hill's condition, i.e. Equation (9), is obtained. Vice versa, if it is assumed that Hill's condition holds true, the stress-averaging formula (8) is obtained.

The following remarks can be made:

1. Equations (5) and (8), i.e. the equality between macroscopic strain or stress and the average on the RVE of the microscopic strain or stress do not make sense when different models are used because the strain and stress measures typically have different meaning and often even different dimensions at the macroscale and the microscale.

2. Equation (2) is meaningless, too, in the general case of two different models used at the two scales. This implies that the definition of the smooth displacement field on the RVE is not necessarily a straightforward issue.

3. Relation (5) certainly applies when uniform boundary conditions are prescribed, see Michel *et al.* [32]. Otherwise it simply becomes an *a priori* assumption which results in restriction (7) for the boundary conditions to be applied on the fluctuating field w. To the authors' knowledge no specific physical or mathematical justification has ever been provided for such assumption in a case different from uniform boundary conditions. However, such an assumption is still not sufficient to fully define the BVP as it is still necessary to make a choice among all possible boundary conditions which satisfy Equation (7), which is typically done on the basis of experience and engineering judgment. Hence, the question arises whether assumption (5) is really necessary to develop a computational homogenisation theory or it is possible to use experience and engineering judgment directly to determine an effective set of boundary conditions for the BVP on the RVE.

4. Unlike Equations (5) and (8), Equation (9) is also meaningful for the general case in which two different models are used at the two scales. This equation can be seen as a scale-bridging variational condition and, if the equations governing the problem at the small scale are the stationary conditions for an energy potential, it becomes a condition of energy equivalence between the micro- and macro-models. On the other hand, Equation (3) can be written also when a potential energy cannot be defined at the small scale, and is therefore more general.

5. Hill's condition (i.e. Equation (9)) was originally derived in the case of uniform displacement or uniform traction boundary conditions [2, 33] (see also Michel *et al.* [32]) and later in the case of periodic boundary conditions by Suquet [34]. However, this equation is normally invoked as an *a priori* assumption of energy equivalence.

These five remarks form a point of departure from which a more general theory in the next section is developed.

2.2 A general framework for homogenisation

In this section we develop a theory to provide and justify the extension of the multi-scale procedure to the case where two different models are used at either scale and no potential energy can be introduced at the small scale. We are particularly interested in the analysis of unbonded flexible risers using the approach described in Ref. [27], in which a co-rotational beam model is used at the macro-scale, while at the small-scale a geometrically linear multi-layered model is used in which each layer is modelled with shell elements and adjacent layers are in potential frictional contact. Therefore, here we consider a two-scale formulation in which a geometrically nonlinear model is used at the macro-scale and a geometrically linear model is adopted at the micro-scale. The extension to the case where geometric nonlinear models are used at both scales is possible within the proposed generalised framework, but it also requires addressing some nontrivial issues regarding the micro-scale formulation, including how to apply and update the boundary conditions, which we prefer to leave for future developments. We also make the hypothesis that body forces are absent.

Apart from the above assumptions, we also wish to make the treatment general enough to be applicable to any other case of computational two-scale homogenisation, when the models used at the two scales are not necessarily continuum models and are generally different from each other. To this end, we use the abstract notation of operators, vector spaces and bilinear forms. In particular, we will indicate the argument of a linear operator without parenthesis, while the argument of a nonlinear operator will be included in parentheses. For example, $b = A(a)$ will be used if operator A is nonlinear, while $b = A\,a$ will be used if A is linear. For a nonlinear operator A, the symbol dA will indicate its derivative, which is always assumed to be properly defined. Furthermore, the adjoint of an operator A will be denoted by A^*.

We consider a macro-scale structural model defined by a vector space $\mathcal{V}_M$ of admissible macro-displacements, a vector space $\mathcal{D}_M$ of admissible macro-strains, and a macro-scale nonlinear strain operator $B_M : \mathcal{V}_M \to \mathcal{D}_M$. We then define a micro-scale structural model defined by vector spaces $\mathcal{V}_m$ and $\mathcal{D}_m$ of admissible micro-displacements and micro-strains, respectively, and a linear strain

operator $B_m : \mathcal{V}_m \to \mathcal{D}_m$. For the purposes of this work, there is no need to specify the functional nature of $\mathcal{V}_M$, $\mathcal{D}_M$, $\mathcal{V}_m$ and $\mathcal{D}_m$, because the determination of mathematical conditions for the existence and uniqueness of the solution, as well as for finite-element convergence and multi-scale convergence, are left for future developments. It is therefore sufficient to assume the elements of $\mathcal{V}_M$ and $\mathcal{D}_M$ are displacement and strain fields (u_M, ε_M) defined in the macro-structural domain Ω, while elements of $\mathcal{V}_m$ and $\mathcal{D}_m$ are displacement and strain fields (u_m, ε_m) defined in $\Omega \times \Omega_{RDE}$, where Ω_{RDE} is the 'representative domain element' independently associated with each point of the macro domain due to the assumption of scale separation, that is carried over into the generalised formulation. The change in notation from RVE to RDE emphasizes that the domain is not necessarily a physical volume. We also assume that the elements of $\mathcal{V}_M$, $\mathcal{D}_M$, $\mathcal{V}_m$ and $\mathcal{D}_m$ and all the required derivatives are sufficiently regular.

Spaces $\mathcal{V}_M, \mathcal{V}_m$ are associated with the dual spaces $\mathcal{F}_M$, $\mathcal{F}_m$, whose elements are external macro- and micro-forces, respectively. These pairs of spaces are related by non-degenerate bilinear forms that have the physical meaning of macroscopic and microscopic external virtual work. Analogously, spaces $\mathcal{D}_M$ and $\mathcal{D}_m$ are associated with dual spaces $\mathcal{S}_M$ and $\mathcal{S}_m$, whose elements represent the macro- and micro- generalised stresses (or stress resultants), respectively. To simplify the notation, the same symbol $(\!(\bullet, \bullet)\!)$ will be used to denote the bilinear forms in $\mathcal{F}_M \times \mathcal{V}_M$, $\mathcal{F}_m \times \mathcal{V}_m$, $\mathcal{S}_M \times \mathcal{D}_M$ and $\mathcal{S}_m \times \mathcal{D}_m$, as the difference in meaning will be clear from the context.

A generally nonlinear constitutive law, $\sigma_m = \sigma_m(\varepsilon_m)$, is defined for the micro-scale structural model. In this context, for simplicity, we assume only that the law is one-to-one and both itself and its derivative are sufficiently regular.

To link the two scales we assume that a displacement-based formulation is used at both scales. An appropriate operator $P : \mathcal{D}_M \to \mathcal{V}_m$ is defined to map microscopic displacements to macroscopic strains. The following restrictions apply to the operator:

1. If $u_m \in \mathrm{Ker}(B_m)$ and $u_m = P(\varepsilon_M)$ then $\varepsilon_M = 0$.

2. The compound operator $B_m P$ must map one (and only one) micro-strain ε_m to each macro-strain ε_M.

The operator P, i.e. the down-scaling procedure, is defined by the solution to the following problem:

Given $\varepsilon_M \in \mathcal{D}_M$, *find* $u_m \in \mathcal{V}_m$ *such that:*

$$\begin{cases} u_m = P(\varepsilon_M) = v_m + w_m \\ v_m = \overline{P}\,\varepsilon_M \\ Q_{bc}\, w_m = 0 \\ (\!(\sigma_m(B_m\, u_m), B_m\, \delta w_m)\!) = 0 \qquad \forall \delta w_m : Q_{bc}\, \delta w_m = 0 \end{cases} \tag{13}$$

Once u_m has been found, $u_m = P(\varepsilon_M)$. In this system of equations $\overline{P}$ defines a linear operator (normally, but not necessarily, in closed form) which 'translates' the macro-scale strain ε_M into a corresponding, 'smooth' micro-displacement field v_m. Q_{bc} is a suitably defined trace operator, such that Equation $(13)_3$ represents a suitably chosen set of linear boundary conditions for the fluctuating displacement field w_m.

Combining operators B_m, P and B_M the compound 'multi-scale' strain operator $B_{MS} = B_m\, P\, B_M$ is obtained, as described schematically in Figure 1. B_{MS} is generally nonlinear, because the constitutive law and operator B_M are generally nonlinear.

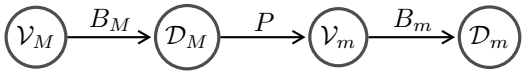

Figure 1: Schematic description of the compound 'multi-scale' strain operator B_{MS}.

B_{MS} and the constitutive law at the small scale fully define a multi-scale structural model, in which $\mathcal{V}_M$ is the vector space of displacements, $\mathcal{D}_m$ is the vector space of strains and $\mathcal{S}_m$ and $\mathcal{F}_M$ are the spaces of generalised stresses and external forces associated with $\mathcal{D}_m$ and $\mathcal{V}_M$ through the appropriate bilinear forms. In theory, the details of the up-scaling procedure could be ignored because what matters are the 'multi-scale' operator B_{MS}, the bilinear forms defined in $\mathcal{F}_M \times \mathcal{V}_M$ and $\mathcal{S}_m \times \mathcal{D}_m$ and the micro-scale constitutive law. Defined in this form, the multi-scale structural model is schematised in Figure 2, where dB^*_{MS} is the adjoint operator to dB_{MS}.

In practice, in many cases it is useful or necessary to consider the spaces $\mathcal{D}_M$ and $\mathcal{S}_M$ explicitly and use an up-scaling procedure to determine the macro-stress field σ_M of $\mathcal{S}_M$ associated with

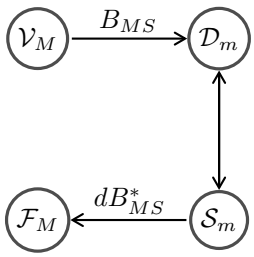

Figure 2: Multi-scale model.

the micro-stress field σ_m.

The up-scaling procedure can be formally obtained from the adjoint operators to B_m and dP as follows:

$$\sigma_M = [dP(\varepsilon_M)]^* \, B^*_m \, \sigma_m \tag{14}$$

This is equivalent to the following variational definition of σ_M:

$$(\!(\sigma_M, \delta\varepsilon_M)\!) = (\!(\sigma_m, B_m \, dP(\varepsilon_M) \, \delta\varepsilon_M)\!) \qquad \forall \delta\varepsilon_M \in \mathcal{D}_M \tag{15}$$

which represents a generalised Hill's condition (GHC). The up-scaling procedure is schematised below in Figure 3.

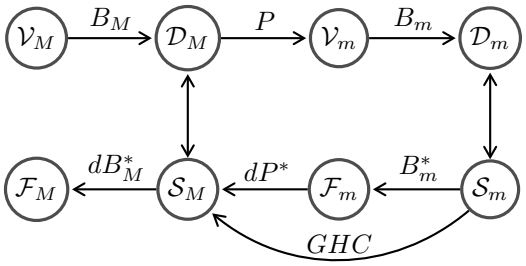

Figure 3: Schematic description of the up-scaling procedure.

The differential $dP(\varepsilon_M)d\varepsilon_M$ of P can be expressed with the aid of Equations $(13)_{1-3}$ as:

$$dP(\varepsilon_M)d\varepsilon_M = \overline{P} \, \delta\varepsilon_M + \delta w_m \tag{16}$$

where $Q_{bc}\,\delta w_m = 0$. Substituting into Equation (15) and noting that Equation $(13)_4$ holds for the variation of the displacement fluctuation field, the following relation is obtained:

$$\langle\!\langle \sigma_M, \delta\varepsilon_M \rangle\!\rangle = \left\langle\!\left\langle \sigma_m, B_m\,\overline{P}\,\delta\varepsilon_M \right\rangle\!\right\rangle \qquad \forall \delta\varepsilon_M \in \mathcal{D}_M \tag{17}$$

Both Equations (15) and (17) define σ_M, but applying them in practice is different: Equation (15) requires the linearisation of the operator P, i.e. of the solution of the micro-problem in the RDE. When such solution is obtained numerically, its linearisation can only be obtained through perturbations, which can be computationally very expensive. Conversely, applying Equation (17) requires only the operators B_m and $\overline{P}$ which are predefined and therefore leads to a direct computation of σ_M.

Furthermore, if problem (13) is practically solved for each RDE using the finite-element method and by introducing ε_M in the micro-problem in the form of degrees of freedom of a dummy control node (see, for example, Michel *et al.* [32]), then Equation (17) is equivalent to recovering σ_M as the reaction of the constraint imposed on this dummy control node.

It is worth noting that the generalised Hill's condition (15) and its simplified form (17), which fully define σ_M and therefore the up-scaling procedure, are not invoked as an *a priori* assumption of the theory. Instead, they are simply derived from the definition of σ_M in terms of duality.

2.2.1 Solution of the micro-problem in terms of u_m

In the above formulation, the total micro-displacement field is found from the sum of $v_m = \overline{P}\,\varepsilon_M$ and the fluctuating field w_m. From the practical point of view this implies assuming w_m as the field variable to be solved for. In a finite-element implementation this implies assuming that the nodal degrees of freedom in the micro-problem represent the nodal values of w_m.

It may be practically convenient, for example when using commercial software packages, to solve the problem directly in terms of u_m, so that in a finite-element implementation the nodal degrees of freedom correspond to the nodal values of u_m. To this end, substituting the relation $w_m = u_m - \overline{P}\,\varepsilon_M$ into Equations (13), and noting that, for a given ε_M, $\delta w_m = \delta u_m$, the micro-problem can be rewritten as follows:

Given $\varepsilon_M \in \mathcal{D}_M$*, find* $u_m \in \mathcal{V}_m$ *such that*

$$\begin{cases} Q_{bc}\, u_m = Q_{bc}\, \overline{P}\, \varepsilon_M \\ (\!(\sigma_m(B_m\, u_m), B_m\, \delta u_m)\!) = 0 \\ \qquad\qquad \forall \delta u_m \,:\, Q_{bc}\, \delta u_m = 0 \end{cases} \tag{18}$$

As mentioned above, in practice dummy control nodes C can be introduced whose degrees of freedom are the components of ε_M for each RDE. This is effectively equivalent to having the micro-problem defined in the product space $\mathcal{V}_m \times \mathcal{D}_M$. Let us denote by $\eta_{MC} \in \mathcal{D}_M$ a vector containing the new degrees of freedom associated with these control nodes, which may be unknown or prescribed. The problem can then be restated as follows:

Given $\varepsilon_M \in \mathcal{D}_M$*, find* $(u_m,\, \eta_{MC}) \in \mathcal{V}_m \times \mathcal{D}_M$ *such that:*

$$\begin{cases} Q_{bc}\, u_m - Q_{bc}\, \overline{P}\, \eta_{MC} = 0 \\ \eta_{MC} = \varepsilon_M \\ (\!(\sigma_m(B_m\, u_m), B_m\, \delta u_m)\!) = 0 \\ \qquad\qquad \forall \delta u_m \,:\, Q_{bc}\, \delta u_m = 0 \end{cases} \tag{19}$$

The fact that the macro-scale stress σ_M is the reaction of the constraint on the control node can be expressed in a variational way as follows:

$$\begin{gathered} (\!(\sigma_M, \delta\eta_{MC})\!) = (\!(\sigma_m, B_m\, \delta u_m)\!) \qquad \forall \delta\eta_{MC} \in \mathcal{D}_M \\ \forall \delta u_m \,:\, Q_{bc}\, \delta u_m = Q_{bc}\, \overline{P}\, \delta\eta_{MC} \end{gathered} \tag{20}$$

The choice of variation δu_m in the above equation is immaterial because, if δu_{m1} and δu_{m2} are two variations such that $Q_{bc}\, \delta u_{m1} = Q_{bc}\, \overline{P}\, \delta\eta_{MC}$ and $Q_{bc}\, \delta u_{m2} = Q_{bc}\, \overline{P}\, \delta\eta_{MC}$, then it results that $Q_{bc}\, \delta(u_{m2} - u_{m1}) = 0$. From Equation (18) this yields $(\!(\sigma_m(B_m\, u_m), B_m\, \delta(u_{m2} - u_{m1}))\!) = 0$, which finally leads to

$$(\!(\sigma_m(B_m\, u_m), B_m\, \delta u_{m1})\!) = (\!(\sigma_m(B_m\, u_m), B_m\, \delta u_{m2})\!) \tag{21}$$

In a finite-element implementation these considerations are purely theoretical, because from the practical point of view σ_M is provided simply by the reactions at the control nodes C, which is

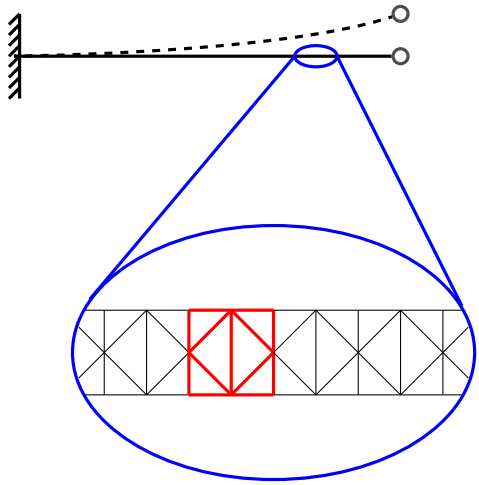

Figure 4: Beam-truss multi-scale model

typically given by the program as part of the standard output.

3 Specialisation to a multi-scale analysis of a truss structure

In this section, an application of the extended multi-scale theory is demonstrated and can be regarded as a template for the application of the extended theory to a wider range of problems. A two-scale model of a slender periodic two-dimensional truss structure is created, using one repeating truss unit as the RDE and employing an Euler-Bernoulli beam model as the large-scale model.

This problem has been chosen to emphasize the generality of the derivation of the extended multi-scale homogenisation theory provided above in Section 2.2. In particular, our formulation is not restricted to structural models obtainable from a continuum model with some kinematic hypotheses. Although each member of a truss structure is a rod and can be derived from a continuum model using some kinematic assumptions, the truss unit forming the RDE used in numerical demonstrations in the following section, shown in Figure 4, is an assembly of rods and therefore cannot be derived in any of the usual ways from a continuum model.

3.1 Large-scale model and definition of $\mathcal{V}_M$, $\mathcal{D}_M$ and B_M

Since, the large-scale model is a slender structure, its kinematic response is modelled using the Euler-Bernoulli beam model. Thus the large-scale domain is

$$\Omega := \{x \in \mathbb{R} : 0 \leq x \leq L\}$$

where L is the model length. The structure is discretised with two-node beam elements with two planar displacements and one rotation as degrees of freedom of each node. To describe how the extended theory of Section 2 specialises to this specific example we prefer to refer directly to the discretised problem. Hence, the space of displacements is defined as $\mathcal{V}_M := \mathbb{R}^{3N_M}$, where N_M is the number of (macroscopic) nodes. Given a displacement $u_M \in \mathcal{V}_M$, u^i_{Mj} will denote the j^{th} component of the i^{th} node. Axial strain and curvature are defined for each element, whereby the strain space is defined as $\mathcal{D}_M := \mathbb{R}^{2N_g E_M}$, where E_M is the number of macroscopic elements and N_g is the number of integration points per element. Given a strain $\varepsilon_M \in \mathcal{D}_M$, ε^{ip}_{Mj} will indicate the j^{th} component of the p^{th} integration point of the i^{th} element. Indicating with ξ the non-dimensional coordinate within a reference unit-length beam element, with end nodes at $\xi = 0$ and $\xi = 1$, the macroscopic strain-displacement operator $B_M : \mathcal{V}_M \to \mathcal{D}_M$ is the nonlinear mapping

$$\begin{aligned} \varepsilon^{ip}_{Mq} = (\hat{B}^i_M)_{qh}(\xi_p)\hat{v}^i_h(\Lambda^i_{kn}v_n) \qquad & i = 1, 2, \dots E_M \qquad n = 1, 2, \dots 3N_M \\ & h, k = 1, 2, \dots 6 \qquad 0 \leq \xi_p \leq 1 \\ & p = 1, 2, \dots N_g \qquad q = 1, 2 \end{aligned} \tag{22}$$

where v_n is the vector of assembled global displacements such that, when $n = 3(i-1)+j$, $v_n = u^i_{Mj}$ $(j = 1, 2, 3)$, ξ_p is the non-dimensional coordinate of the pth integraton point, Λ^i_{kn} is the incidence matrix and $\hat{v}^i_h$ is the hth component of the local displacements for element i, which is a nonlinear function of the global element displacement components $v^i_k = \Lambda^i_{kn}v_n$. The

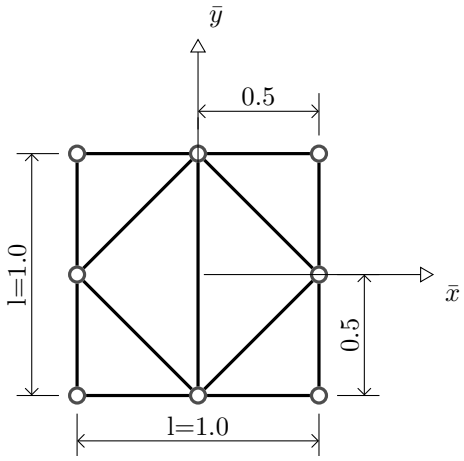

Figure 5: Geometry of the RDE (dimensions in m)

nonlinear mapping $\hat{v}_h^i = \hat{v}_h^i(v_k^i)$ is defined in the corotational formulation developed by Urthaler and Reddy [35] that is adopted here. Furthermore, $\hat{B}_M^i$ is the strain-displacement matrix

$$\hat{B}_M^i(\xi) = \frac{1}{l_i^2}\begin{bmatrix} -l_i & 0 & 0 & l_i & 0 & 0 \\ 0 & 12\xi - 6 & (6\xi - 4)l_i & 0 & -12\xi + 6 & (6\xi - 2)l_i \end{bmatrix}$$

where l_i is the length of beam element i. The incidence matrix is defined as

$$\Lambda_{kn}^i = \begin{cases} 1 & \text{if global DOF } n \text{ corresponds to element DOF } k \text{ of element } i \\ 0 & \text{otherwise} \end{cases}$$

noting that element DOFs represent the planar translational displacements and rotation of the nodes of the element using the ordering $(u_1^1, u_2^1, u_3^1, u_1^2, u_2^2, u_3^2)$, as does the global displacement vector v_n.

3.2 Small-scale model and definition of $\mathcal{V}_m$, $\mathcal{D}_m$ and B_m

The small-scale model consists of 2-noded planar truss elements. Elastoplastic material behaviour with linear kinematic hardening is chosen for the constitutive relation of the members.

No finite-element approximation is required because the small-scale model is already finite-dimensional in nature and consists of N_m nodes and E_m elements. The space of displacements is defined as $\mathcal{V}_m := \mathbb{R}^{2N_g E_M 2N_m}$. Focusing on a single integration point, given a displacement u_m, u^i_{mj} will denote the j^{th} component of the i^{th} node. The space of strains is defined as $\mathcal{D}_m := \mathbb{R}^{2N_g E_M E_m}$. Focusing on a single integration point, given a strain $\varepsilon_m \in \mathcal{D}_m$, ε^i_m is the axial strain of the i^{th} element.

$B_m : \mathcal{V}_m \to \mathcal{D}_m$ is the linear mapping that, for each RDE, is defined as follows:

$$\varepsilon^i_m = \hat{B}^i_{mh} T^i_{hk} \Lambda^i_{kn} v_n \qquad i = 1, 2, \ldots E_m \qquad n = 1, 2, \ldots 2N_m$$
$$h, k = 1, 2, \ldots 4 \tag{23}$$

where v_n is the vector of assembled global displacements such that, when $n = 2(i-1) + j$, $v_n = u^i_j$ $(j = 1, 2)$, Λ^i_{kn} is the incidence matrix, l_i is the length of truss element i and T^i_{hk} is the 2D coordinate transformation matrix for element i.

The strain-displacement matrix is:

$$\hat{B}^i_m = \frac{1}{l_i} \begin{bmatrix} -1 & 0 & 1 & 0 \end{bmatrix}$$

The incidence matrix is as defined in Section 3.1, noting that element DOFs represent the planar translational displacements of the nodes of the element using the ordering (u^1_1, u^1_2, u^2_1, u^2_2), as does the assembled displacement vector.

3.3 Scale bridging and definition of $\bar{P}$ and Q_{bc}

For these models, the operator $\bar{P} : \mathbb{R}^{2N_g E_M} \to \mathbb{R}^{2N_g E_M 2N_m}$ is defined in accordance with the Euler-Bernoulli kinematic assumptions as follows.

Given a node n of the small-scale truss model, the two components of the displacement of node n in the local directions $\bar{x}$ and $\bar{y}$ (see Figure 5) are given by:

$$v_{n\bar{x}} = \alpha_M^{ip}\bar{x}_n + \chi_M^{ip}\bar{x}_n\bar{y}_n$$

$$v_{n\bar{y}} = 0.5\chi_M^{ip}\bar{x}_n^2 \tag{24}$$

where $\bar{x}_n$ and $\bar{y}_n$ are the local coordinates of n, while α_M^{ip} and χ_M^{ip} are the axial strain and curvature at the corresponding integration point p of element i.

Denoting by N_b the number of nodes on the small-scale model's left boundary, which is equal to the number of nodes on the right boundary, the restriction $Q_{bc}^* : \mathbb{R}^{2N_m} \rightarrow \mathbb{R}^{2N_b}$ of operator Q_{bc} in Equations (18), (19), (20) and (21) to a single RDE is defined as follows:

$$(Q_{bc}^*)_{ij} = \begin{cases} 1 & \text{if degree of freedom } j \text{ corresponds to degree of freedom } i \\ & \quad \text{on right boundary} \\ -1 & \text{if degree of freedom } j \text{ corresponds to degree of freedom } i \\ & \quad \text{on left boundary} \\ 0 & \text{otherwise} \end{cases}$$

$$i = 1, 2, \ldots 2N_b \qquad j = 1, 2, \ldots 2N_m$$

We choose to apply the macroscopic strains to the microscopic model by means of a dummy control node, as described in Equation (19).

3.4 Multi-scale implementation

The large-scale model was implemented in the finite-element package Abaqus using user-defined elements to calculate the response of the small-scale model. The small-scale model and the scale bridging procedure were implemented as the material model used within the UEL subroutine. Three integration points were used for each large-scale element. For each integration point three simulations were carried out for each iteration of each increment of a full Newton-Raphson solution procedure. The macro-strain was passed for the first simulation to compute the macro-stress and perturbations of each of the two macro-strain components were passed in the remaining

two simulations to compute the associated macro-stress variation and establish the consistent material tangent.

4 Numerical results

4.1 Test case

In this section we numerically test convergence of the multi-scale procedure, or, in short, multi-scale convergence. By multi-scale convergence, we mean that the difference between the multi-scale solution and direct numerical simulation (DNS) results tends to zero as the ratio ϵ between the characteristic lengths of the unit cell and the large-scale model tends to zero. This is investigated for the case of a truss structure created using a periodic array (Figure 4) of the unit cell truss structure shown in Figure 5. For the small-scale model the characteristic length is 1m. For the large-scale model it is the total length of the structure L.

To separate multi-scale convergence from FE convergence, for each case analysed we present results for increasing numbers of elements of the large-scale model. For the small-scale model this is not necessary because it is already discrete in nature.

Model parameters (with reference to Section 3) are presented in Table 1.

Three cases were studied for this type of structure. For case 1, a cantilever truss with an axial point load at the end of the structure was considered (Figure 6). For case 2, a transverse point load was applied to the same cantilever truss (Figure 7). For case 3, a point load was applied to the left-hand span of a truss beam with three simple supports (Figure 8).

Figures 6-8 show geometry and loading for the three cases, referring to the multi-scale analysis, whereby the structure is modelled as a beam.

Each of these cases was modelled by both DNS, which account for large displacements and rotations of the truss members, and the fully nested (FE^2) multi-scale procedure. For the latter, the multi-scale procedure described in Section 3 was used. For each case, four values of the length L have been considered: 20, 60, 100 and 400m. Since the length of the RDE is 1m (Figure 5), the four different lengths correspond to four values of the scaling parameter $\epsilon = l/L$, equal

Model parameters	
Load magnitude (for axial loading)	2×10^7 N
Load magnitude (for transverse loading)	$4 \times 10^5 \times \left(\frac{L}{20}\right)$ N
Load magnitude for statically indeterminate load case	$4.3788 \times 10^6 \times \left(\frac{L}{20}\right)$ N
Young's modulus	200×10^9 Nm^{-2}
Yield limit	400×10^6 Nm^{-2}
Kinematic hardening constant	100×10^9 Nm^{-2}
Member cross-sectional area	0.01 m^2

Table 1: Material parameters

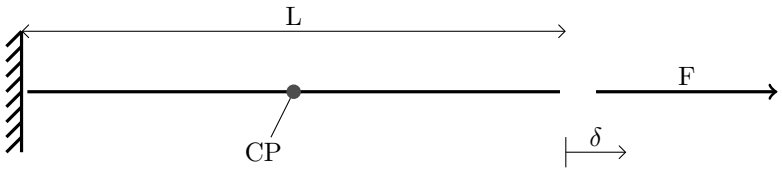

Figure 6: Case 1: Macro-geometry and loading. Comparison point (CP) located at distance 0.5L from support.

to 0.05, 0.016667, 0.01 and 0.0025.

For each study, multi-scale convergence was evaluated by comparing the DNS results with those of the multi-scale analysis for each value of ϵ. For each value of ϵ, finite-element convergence of the multi-scale model with increasing number of elements was also examined.

4.2 Results

Convergence results for case 1 are shown in Figures 9 and 10. Results for case 2 are shown in Figures 11 and 12. Results for the case 3 are shown in Figures 13 and 14.

Displacement results were evaluated at the node corresponding to the comparison point (shown in Figures 6-8). For the DNS, stress results were obtained by averaging stresses in the two horizontal members on either side of the comparison point on the underside of the truss. For the multi-scale simulations, the comparison point is a node, and stress results are the average

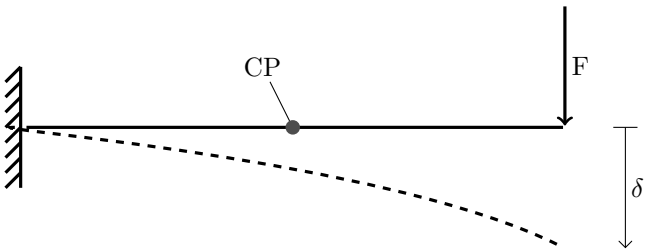

Figure 7: Case 2: Macro-geometry and loading. Comparison point (CP) located at distance 0.5L from support.

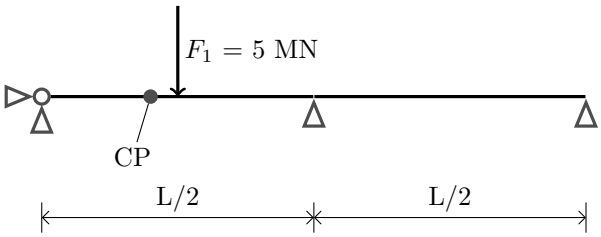

Figure 8: Case 3: Macro-geometry and loading. Comparison point (CP) located at distance 0.2L from pin joint; applied load located at distance 0.25L from pin joint.

of the two integration points in the large-scale model on either side of the comparison point. For each integration point, the stresses in the horizontal truss members on the lower side of the RDE were evaluated. Due to the symmetry of the RDE problem, both lower horizontal members show the same stress.

Tolerances of 10^{-8}, 10^{-5} and 10^{-5} for the relative residual norm error were used for the DNS solver, the large-scale solver and the small-scale solver, respectively. The minimum error that can be achieved in these simulations is closely linked with the maximum tolerance used of 10^{-5}.

For case 1, Figures 9 and 10 show that both displacement and stress in the multi-scale model do not depend on the number of elements, whereby FE convergence is not an issue. Displacement results become increasingly accurate as the scaling parameter ϵ increases, showing multi-scale convergence. Stress results do not change as the error is already as low as the numerical tolerance will allow.

For case 2 (Figures 11 and 12) displacement results from the multi-scale analysis are not

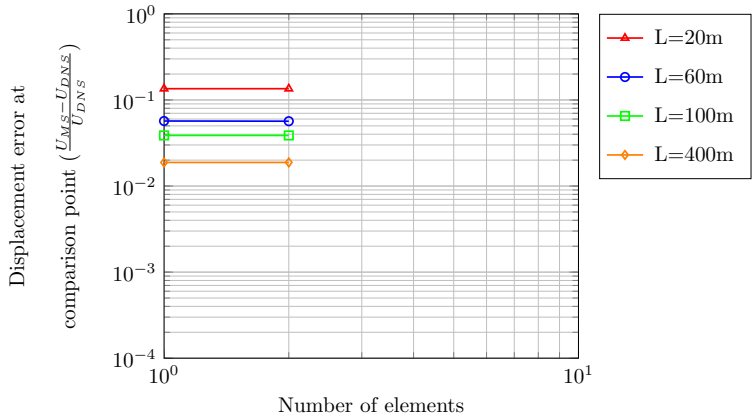

Figure 9: Multi-scale and FE displacement convergence at the comparison point for the axially loaded cantilever (case 1)

significantly affected by number of elements. FE convergence appears to be achieved for L=60m and L=100m, which are more important to assess multi-scale convergence. With decreasing ϵ multi-scale convergence can be observed for displacement results. For stresses the error for the multi-scale analysis is already below 0.2% for L=20m and only slightly reduces from L=60m to L=100m because the numerical tolerance has been reached. Increasing the number of elements does not significantly reduce error if more than 40 elements are used, showing that finite element convergence has occurred. For L=400, the Newton-Raphson procedure used did not converge.

For case 3, which is statically indeterminate (Figures 13 and 14), neither displacement nor stress results are significantly affected by the number of elements. Both stress and displacement results converge as ϵ is decreased. The displacement error for the multi-scale procedure decreases from about 9% for L=20m to less that 0.5% for L=100m.

Deformed figures for transverse loading and the statically indeterminate load cases are shown in Figures 15, 16, 17 and 18, highlighting that the extent of plastic zones is constant with varying model length.

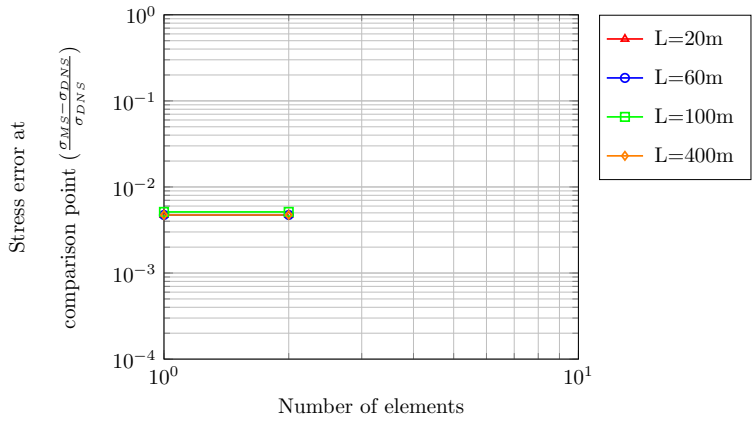

Figure 10: Multi-scale and FE stress convergence at the comparison point for the axially loaded cantilever (case 1)

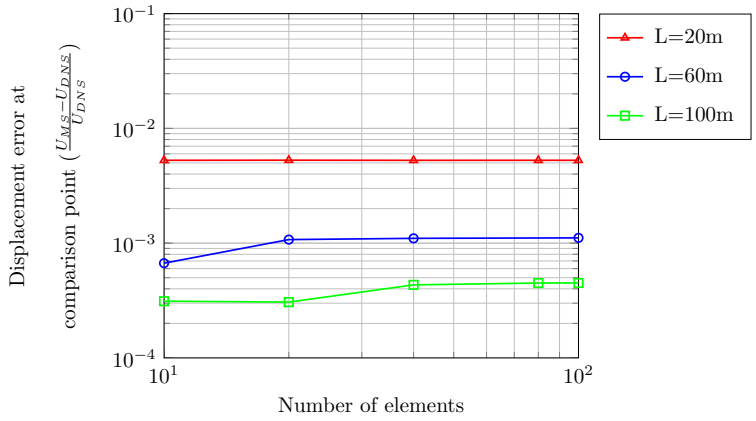

Figure 11: Multi-scale and FE displacement convergence at the comparison point for the transversally loaded cantilever (case 2)

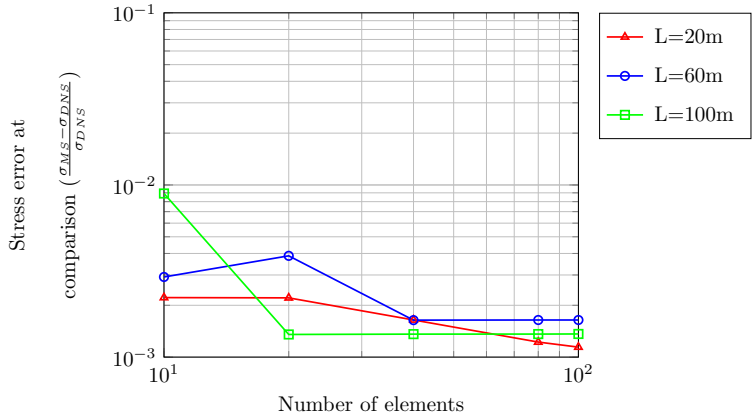

Figure 12: Multi-scale and FE stress convergence at the comparison point for the transversally loaded cantilever (case 2)

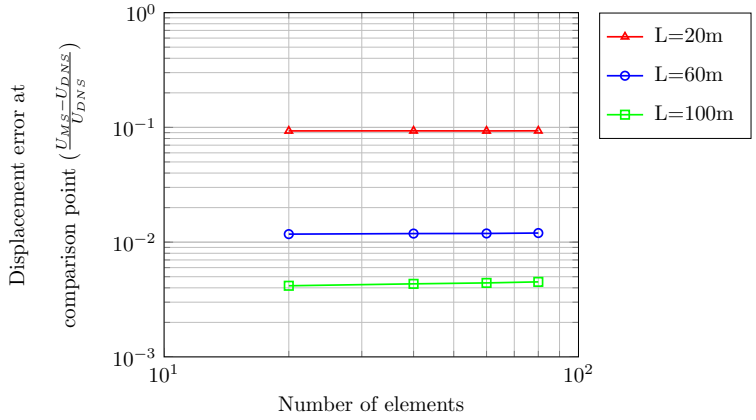

Figure 13: Multi-scale and FE displacement convergence at the comparison point for the statically indeterminate load case (case 3)

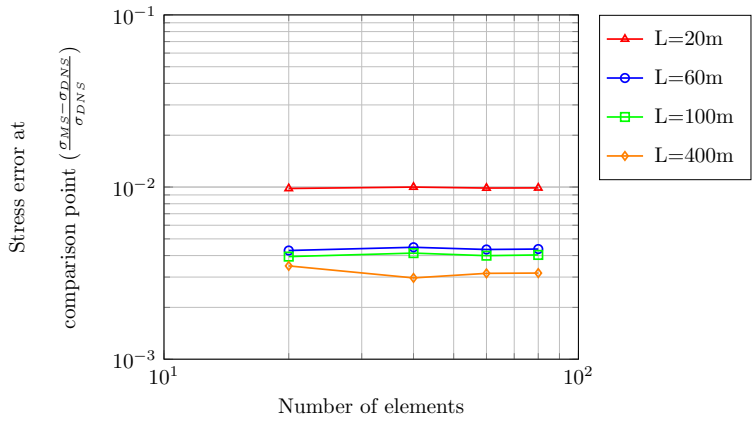

Figure 14: Multi-scale and FE stress convergence at the comparison point for the statically indeterminate load case (case 3)

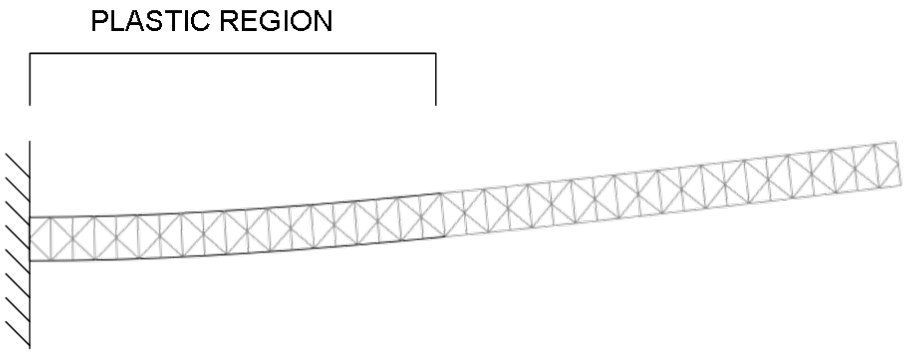

Figure 15: Material state for transverse loading, L=20m. Elements with stress greater than yield limit are black; elements with stress under yield limit are grey.

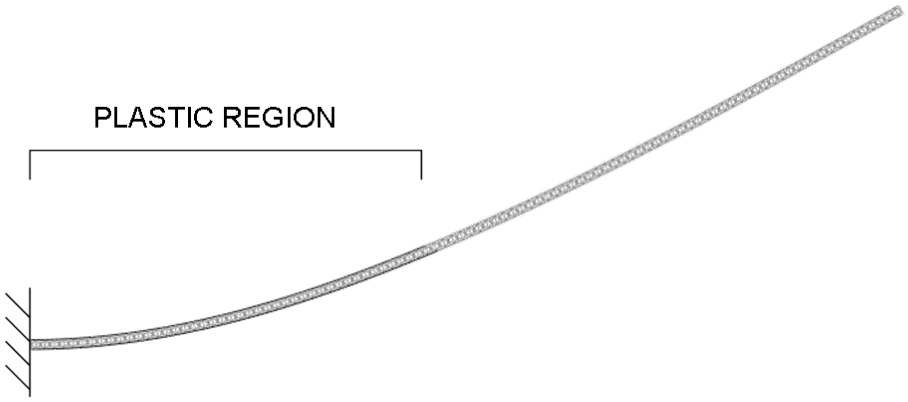

Figure 16: Material state for transverse loading, L=100m. Elements with stress greater than yield limit are black; elements with stress under yield limit are grey.

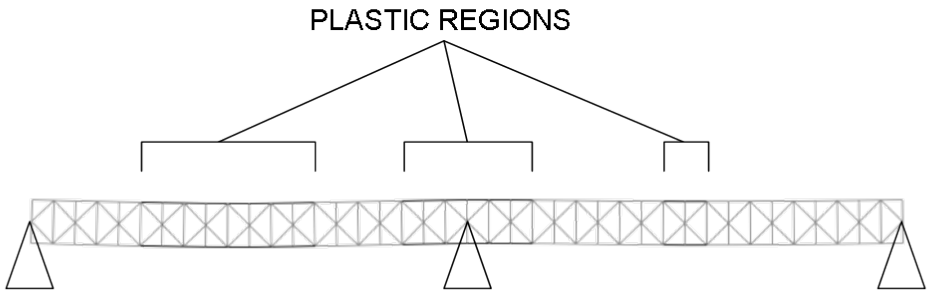

Figure 17: Material state for statically indeterminate load case, L=20m. Elements with stress greater than yield limit are black; elements with stress under yield limit are grey.

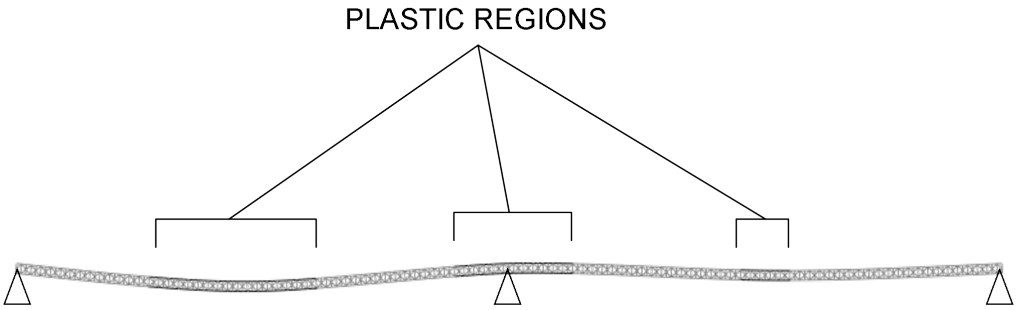

Figure 18: Material state for statically indeterminate load case, L=100m. Elements with stress greater than yield limit are black; elements with stress under yield limit are grey.

5 Conclusions

We presented a nonlinear computational homogenisation theory which can be directly applied to cases in which different structural models are used at different length scales, whereby volumetric averaging principles are not applicable, and where the lower-scale problem is not necessarily governed by an energy potential.

An original and more general theoretical justification of how the micro-scale BVP is defined starting from the macro-strain was provided. In our generalised formulation we introduced at each point of the macro domain a representative domain element (RDE) instead of a RVE, because our theory is not restricted to solid continua. We revisited the conventional point of departure that the RDE average of the micro-strains has to be equal to the macro-strain, which is not applicable to the general case as a means of deriving appropriate boundary conditions for the RDE. In particular, we observed that not only is this assumption unnecessary but it is also insufficient to define a well-posed micro-scale BVP. Instead, we showed that to construct a general theory that is applicable regardless of the structural models used at either scale it is sufficient to introduce a linear operator, which maps the 'smooth' part of the micro-displacement field in the RDE to the macro-strain, as well as a suitably defined trace operator that imposes

boundary conditions on the RDE, the latter to be defined based on engineering judgement. As a physically realistic choice of boundary conditions is also a required input for conventional computational homogenisation procedures, this does not represent a limitation of our approach. The up-scaling procedure used to recover the stress field in the large-scale model is based upon a generalised Hill's condition, which is not invoked as an *a priori* assumption but is obtained from general duality principles.

Instead of using volumetric averaging to transfer quantities between small and large scales, the small-scale model is augmented with additional degrees of freedom corresponding to the large-scale strains, allowing both the imposition of strains and the recovery of stresses via linear constraint equations.

For the sake of simplicity but also driven by our interest for the analysis of flexible risers, in this paper our formulation has been developed for cases where a geometrically linear model is used at the small scale, whereas a geometrically nonlinear model is used at the large scale. However, the principles can be be extended to the general case where geometrical nonlinearity is accounted for at both scales, which will be addressed in future work.

An application of the method to the nonlinear multi-scale analysis of truss structures has been presented. This type of problem has been chosen because it cannot be analysed by applying existing methods proposed in the literature because different models are used at different scales and because the small-scale model (the truss) is not recoverable from a continuum model. Furthermore, due to the very low computational cost of the small-scale model direct numerical simulations (DNS) can be performed, which allowed us to study and discuss multi-scale convergence for three loading conditions.

The extension of computational homogenisation to structural-to-structural multi-scale models enables new approaches to material and structural modelling problems bridging length scales to be implemented and could allow the rapid creation of multi-scale models using combinations of simple structural elements such as springs, dampers, frictional sliders and thermal expansion elements to represent local behaviour. Where constitutive models are complex, such structural-to-structural multi-scale could be significantly more efficient than continuum multi-scale models

due to dimensional reduction.

We suggest that the computational homogenisation method outlined in this article could be a fruitful approach to modelling problems including marine flexible risers, auxetic materials, honeycomb structures or other impact attenuation materials like foams. Further work is also needed to address the mathematical conditions for the existence and uniqueness of the multi-scale solution and for multi-scale convergence.

Acknowledgements

The authors wish to acknowledge gratefully the financial support and technical advice provided by Lloyd's Register EMEA.

References

[1] Hashin Z. Analysis of composite materials - a survey. *Journal of Applied Mechanics - Transactions of the ASME* September 1983; **50**(3):481–505.

[2] Hill R. Elastic properties of reinforced solids: Some theoretical principles. *J. Mech. Phys. Solids* 1963; **11**(5):357–372.

[3] Yuan Z, Fish J. Toward realization of computational homogenization in practice. *International Journal for Numerical Methods in Engineering* 2008; **73**(3):361–380.

[4] Matsui K, Terada K, Yuge K. Two-scale finite element analysis of heterogeneous solids with periodic microstructures. *Computers and Structures* 2004; **82**(7–8):593–606.

[5] Perić D, de Souza Neto EA, Feijóo RA, Partovi M, Molina AJC. On micro-to-macro transitions for multi-scale analysis of non-linear heterogeneous materials: Unified variational basis and finite element implementation. *International Journal for Numerical Methods in Engineering* 2011; **87**(1–5):149–170.

[6] Terada K, Hori M, Kyoya T, Kikuchi N. Simulation of the multi-scale convergence in computational homogenization approaches. *International Journal of Solids and Structures* 2000; **37**(16):2285–2311.

[7] Amieur M, Hazanov S, Huet C. Numerical and experimental assessment of the size and boundary conditions effects for the overall properties of granular composite bodies smaller than the representative volume. *IAUTAM Symposium on Anisotropy, Inhomogeneity and Nonlinearity in Solid Mechanics*, Parker D, England A (eds.), Kluwer Academic Publishers: Dordrecht, 1995; 149–154.

[8] Hazanov S, Huet C. Order relationships for boundary conditions effect in heterogeneous bodies smaller than the representative volume. *J. Mech. Phys. Solids* 1994; **42**(12):1995–2011.

[9] van der Sluis O, Schreurs PJG, Brekelmans WAM, Meijer HEH. Overall behaviour of heterogeneous elastoviscoplastic materials: Effect of microstructural modelling. *Mechanics of Materials* 2000; **32**(8):449–462.

[10] Somer DD, de Souza Neto E, Dettmar WG, Perić D. A sub-stepping scheme for multi-scale analysis of solids. *Comput. Methods Appl. Mech. Engrg.* 2009; **198**(9–12):1006–1016.

[11] Kouznetsova V, Geers M, Brekelmans W. Multi-scale constitutive modelling of heterogeneous materials with a gradient-enhanced computational homogenization scheme. *International Journal for Numerical Methods in Engineering* 2002; **54**(8):1235–1260.

[12] Kaczmarczyk Ł, Pearce C, Bićanić N, de Souza Neto E. Numerical multiscale solution strategy for fracturing heterogeneous materials. *Computer Methods in Applied Mechanics and Engineering* 2010; **199**(17–20):1100–1113.

[13] Addessi D, Sacco E, Paolone A. Cosserat model for periodic masonry deduced by nonlinear homogenization. *European Journal of Mechanics A/Solids* 2010; **29**(4):724–737.

[14] Addessi D, Sacco E. A multi-scale enriched model for the analysis of masonry panels. *International Journal of Solids and Structures* 2012; **49**(6):865–880.

[15] Geers M, Coenen E, Kouznetsova V. Multi-scale computational homogenization of structured thin sheets. *Modelling and Simulation in Materials Science and Engineering* 2007; **15**(4):393–404.

[16] Coenen EWC, Kouznetsova VG, Geers MGD. Computational homogenization for heterogeneous thin sheets. *International Journal for Numerical Methods in Engineering* August 2010; **83**(8–9):1180–1205.

[17] Samadikhah K, Larsson R, Bazooyar F, Bolton K. Continuum-molecular modelling of graphene. *Computational Materials Science* 2012; **53**(1):37–43.

[18] Pinho-da-Cruz J, Oliviera JA, Teixeira-Dias F. Asymptotic homogenisation in linear elasticity. Part I: Mathematical formulation and finite element modelling. *Computational Materials Science* 2009; **45**(4):1073–1080.

[19] Hassani B, Hinton E. A review of homogenization and topology optimization: I- Homogenization theory for media with periodic structure. *Computers and Structures* 1998; **69**(6):707–717.

[20] Guedes J, Kikuchi N. Preprocessing and postprocessing for materials based on the homogenization method with adaptive finite element methods. *Computer Methods in Applied Mechanics and Engineering* 1990; **83**(2):143–198.

[21] Ghosh S, Lee K, Moorthy S. Multiple scale analysis of heterogeneous elastic structures using homogenization theory and Voronoi cell finite element method. *Int. J. Solids Structures* 1995; **32**(1):27–62.

[22] Fish J, Shek K. Multiscale analysis of composite materials and structures. *Composites Science and Technology* 2000; **60**(12–13):2547–2556.

[23] Buannic N, Cartraud P. Higher-order effective modeling of periodic heterogeneous beams. I. Asymptotic expansion method. *International Journal of Solids and Structures* 2001; **38**(40–41):7139–7161.

[24] Terada K, Kikuchi N. A class of general algorithms for multi-scale analyses of heterogeneous media. *Comput. Methods Appl. Mech. Engrg.* 2001; **190**(40–41):5427–5464.

[25] Alfano G, Bahtui A, Bahai H. Numerical derivation of constitutive models for unbonded flexible risers. *International Journal of Mechanical Science* 2009; **51**(4):295–304.

[26] Bahtui A, Alfano G, Bahai H, Hosseini-Kordkheili S. On the multi-scale computation of un-bonded flexible risers. *Engineering Structures* 2010; **32**(8):2287–2299.

[27] Edmans B, Alfano G, Bahai H. Multiscale modelling of flexible pipes with nonlinear homogenisation. *Proceedings of the ASME 2010 29th International Conference on Ocean, Offshore and Arctic Engineering*, 2010.

[28] Tollenaere H, Caillerie D. Continuous modelling of lattice structures by homogenization. *Advances in Engineering Software* 1998; **29**(7–9):669–705.

[29] Smith CW, Grima JN, Evans KE. Novel mechanism for generating auxetic behaviour in reticulated foams: Missing rib foam model. *Acta Materialia* 2000; **48**(17):4349–4356.

[30] Larsson F, Runesson K, Saroukhani S, Vafadari R. Computational homogenization based on a weak format of micro-periodicity for RVE-problems. *Computer Methods in Applied Mechanics and Engineering* 2011; **200**(1–4):11–26.

[31] Hazanov S, Amieur M. On overall properties of elastic heterogeneous bodies smaller than the representative volume. *Int. J. Engrg. Sci.* 1995; **33**(9):1289–1301.

[32] Michel JC, Moulinec H, Suquet P. Effective properties of composite materials with periodic microstructure: a computational approach. *Comput. Methods Appl. Mech. Engrg.* 1999; **172**(1–4):109–143.

[33] Hill R. On constitutive macro-variables for heterogeneous solids at finite strain. *Proc. R. Soc. Lond. A*. 1972; **326**(1565):131–147.

[34] Suquet P. Introduction. *Homogenization Techniques for Composite Media*, *Lecture Notes in Physics*, vol. 272, Sanchez-Palencia E, Zaoui A (eds.). Springer Berlin / Heidelberg, 1987; 193–198.

[35] Urthaler Y, Reddy J. A corotational finite element formulation for the analysis of planar beams. *Communications in Numerical Methods in Engineering* 2005; **21**(10):553–570.